



ELSEVIER

Contents lists available at ScienceDirect



## Analytical prediction of floating floors impact sound insulation including thickness-resonance wave effects

Charlotte Crispin <sup>a</sup>, Arne Dijckmans <sup>a</sup>, Debby Wuyts <sup>a</sup>, Andrea Prato <sup>b</sup>, Pierluigi Rizza <sup>b</sup>, Alessandro Schiavi <sup>b,\*</sup><sup>a</sup> Buildwise, Kleine Kloosterstraat 23, B-1932 Zaventem, Belgium<sup>b</sup> INRIM – National Institute of Metrological Research, Applied Metrology and Engineering Division, Strade Delle Cacce 91, 10135 Torino, Italy

## ARTICLE INFO

## Article history:

Received 20 January 2023

Received in revised form 2 March 2023

Accepted 8 April 2023

Available online 13 April 2023

## Keywords:

Impact sound insulation

Thickness resonance waves

Dynamic stiffness

Harrison-Sykes-Martin model

## ABSTRACT

The floating floor technology in buildings is increasingly used to achieve national acoustic and thermal insulation requirements, combining different compositions of materials and components with proper technical features. However, the analytical models nowadays available do not allow to estimate with the due accuracy the actual acoustic performance of floating floors with a thick or heavy resilient layer from involved material properties. The physical model presented in this paper, based on the vibration transmissibility theory, improves the prediction of the effect of a floating screed on the impact sound insulation, as a function of frequency, by taking into account the thickness-resonance wave effects in the resilient layer. The model is based on the exact analytical solution of the one-dimensional wave equation in elastic media. Theoretical results are compared with existing computational models and with experimental data of impact sound insulation.

© 2023 Elsevier Ltd. All rights reserved.

### 1. Introduction

In building physics, the development of materials and components for integrated acoustic-thermal insulation in floors, requires improved and reliable computational models, allowing to accurately define the technical performance of complex systems, in order to address suitable solutions for noise protection, from design to application. Impact sound insulation was largely investigated during the last decades: the simplified Cremer-Vér computational model [1,2] is commonly used to estimate the acoustical behavior of floating floors (e.g., in the ISO 12354-2 Standard [3]). In addition, a constitutive model, based on the vibration transmissibility theory in single-degree-of-freedom systems [4] has been successfully applied to simple floating floor systems [5,6], accurately estimating the amplification around the mass-spring resonance frequency of the system and the damping effects on the impact sound insulation improvement. However, the transmissibility model provides reliable estimations of impact sound insulation, only if the thickness of the resilient material is negligible with respect to the wavelength of longitudinal waves present in the resilient material. If the longitudinal wavelength is of the same order of magnitude as the thickness in the frequency range of interest, the inner field of standing waves in the elastic component,

generates “harmonics” able to reduce the insulation effectiveness. For thermal-acoustic insulation layers used in floating floors, this phenomenon of thickness-resonances can already be observed from 500 Hz upwards [7]. Also for floating floors with heavy resilient layers (e.g. rubber-based), thickness resonances can be observed in the frequency range of interest (<5000 Hz).

Back in 1952, while Cremer [1] formulated the computational model based on parallel-plate coupled with elastic interlayers, Harrison, Sykes and Martin [8] studied the effects of standing waves in bulky insulation mounts, used in systems for vibrations isolation. The Harrison-Sykes-Martin (H-S-M) model [9], although built on the basis of some approximations and limitations of the boundary conditions, provides a very reliable assessment of a mass-spring-damper system motion subjected to harmonic driving forces, by identifying the onset of standing waves within the thick or heavy resilient insulating material, as a function of its inertial, elastic and dissipative properties, and as a function of the floating screed mass applied. Derivations and peculiar applications of the H-S-M formula are usually implemented in applied mechanics for vibration control [10,11]. In the following, the formula is revised and applied to evaluate, as a function of frequency, the improvement of impact sound insulation  $\Delta L$  of floating floors built with thick and heavy resilient layers. Predictions are then compared with experimental results of improvement of impact sound insulation  $\Delta L$ , measured in laboratory, and with existing computational models.

\* Corresponding author.

E-mail address: [a.schiavi@inrim.it](mailto:a.schiavi@inrim.it) (A. Schiavi).

## 2. Force transmissibility models for floating floors

The application of floating floors in buildings allows to reduce vibrations and structure-borne sound transmission between dwellings, reducing the noise annoyance. The basic concept is founded on the decoupling of structural elements by means of continuous resilient layers. The acoustical performance of floating floors is evaluated in laboratory, according to the ISO 10140 Standard series [12], in terms of the improvement of impact sound insulation,  $\Delta L$ .

Several empirical models allow to estimate the improvement of impact sound insulation  $\Delta L$  of a floating floor from the inertial and the elastic properties of the system. As a first approximation, a floating floor can be considered as a single-degree-of-freedom mass-spring mechanical system. The vibration velocity level, resulting from an applied force, is related to the radiated sound pressure level, according to the reciprocity principle [13]. The reduction of the vibrations amplitude, generated by the impacts on the floating screed (i.e., the input force,  $F_{in}$ ) and transmitted to the base floor through the resilient layer, is quantified in terms of force transmissibility insertion loss, according to Eq. (1):

$$\Delta L = 20 \log |F_{in}/F_{out}| = 20 \log |1/\mathcal{T}| \quad (1)$$

where  $F_{out}$  is the resulting amplitude of force transmitted on the base floor and  $\mathcal{T}$  is the constitutive equation of the physical model adopted. This model is intended for floating floors built with highly damped (or “locally reacting”) floating screeds. If the floating screeds are lightly damped (or “resonantly reacting”), relation (1) can simply be rewritten as  $\Delta L = 15 \log |1/\mathcal{T}|$  [2].

In the following a distinction is made between floating floors with acoustically thin and acoustically thick resilient layers.

### 2.1. Floating floors with an acoustically thin resilient layer

In Fig. 1, a schematic illustration of an ordinary floating floor built with a single resilient layer is depicted. When the resilient layer can be considered acoustically thin in the frequency range of interest, i.e. when the longitudinal wavelength in the resilient material is much larger than the thickness of the resilient layer, the system can be modelled as a single-degree-of-freedom mass-spring-damper system, where  $s$  ( $N m^{-3}$ ) is the dynamic stiffness of the resilient layer,  $c$  is the damping coefficient ( $kg s^{-1}$ ) and  $M$  ( $kg m^{-2}$ ) is the actual mass per unit area of the floating screed.

The force transmissibility for this system is given by [14]:

$$\mathcal{T} = \frac{F_{out}}{F_{in}} = \frac{-\frac{js}{\omega} + c}{j\omega M - \frac{js}{\omega} + c} = \frac{j - \frac{c\omega}{s}}{j(1 - \frac{\omega^2}{\omega_0^2}) - \frac{c\omega}{s}} \quad (2)$$

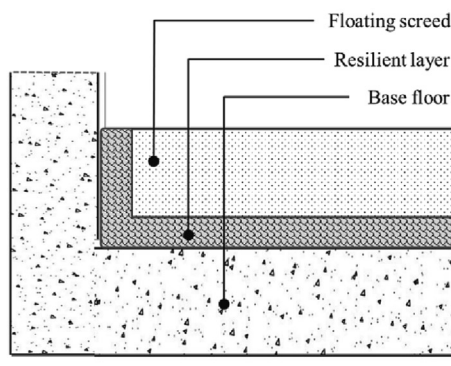


**Fig. 1.** Section of a floating floor built on a concrete base floor, with the floating screed (mass per unit area  $M$ ), and the resilient layer (dynamic stiffness  $s$ ) and damping (dampener of dissipative constant  $c$ ), and the related mechanical model.

where  $\omega_0 = \sqrt{\frac{s}{M}}$  is the mass-spring-resonance frequency of the system. Using the loss factor  $\eta = 2 \frac{c}{c_c} = \frac{c}{m\omega_0}$ , the improvement of impact sound insulation based on the force transmissibility theory, becomes:

$$\Delta L = 20 \log \sqrt{\frac{\eta^2 \left(\frac{\omega}{\omega_0}\right)^2 + \left(1 - \frac{\omega^2}{\omega_0^2}\right)^2}{1 + \eta^2 \left(\frac{\omega}{\omega_0}\right)^2}} \quad (3)$$

In this model, viscous damping is assumed. The force transmissibility and impact sound insulation improvement will therefore be dependent on the loss factor also at higher frequencies. Generally, the damping in floating floors is better described as hysteretic [14], using a complex dynamic stiffness  $s = s(1 + j\eta)$ . In this case, the improvement of impact sound insulation becomes independent of loss factor at higher frequencies:

$$\Delta L = 20 \log \sqrt{\frac{\eta^2 + \left(1 - \frac{\omega^2}{\omega_0^2}\right)^2}{1 + \eta^2}} \quad (4)$$

The constitutive model has been successfully applied to several thin-component floating floors [5,6], with accuracy and reliability, and it has been exploited in advanced impact sound insulation investigations, design and applications [15–20]. Nevertheless, for floating floors with thick or heavy resilient layers, the transmissibility models of Eqs. (3)–(4) do not provide useful and reliable estimations of the actual acoustical behavior in the entire frequency range of interest, because thickness resonances occurring in the resilient layer can significantly reduce the improvement of impact sound insulation, even in the middle frequency range [7]. In the following section, the original H-S-M model for vibration isolators is revised and applied to floating floors with acoustically thick resilient layers.

### 2.2. Floating floor with an acoustically thick resilient layer

The theoretical foundation of the proposed model deals with traveling and standing waves in resilient materials. These waves are a combination of compression, shear, bulk, torsion and surface waves, having the ability to impair the noise insulation properties of the resilient element within the floating floor, increasing the force transmissibility, particularly at high frequencies, due to the onset of resonant peaks.

Assuming a one directional harmonic driving force (along the vertical  $x$ -axis),  $F_{in} = F e^{j\omega t}$ , and hysteretic damping, the travelling motion of the longitudinal waves in the resilient layer is given by:

$$\begin{aligned} F_{in} &= F e^{j\omega t} \\ &\downarrow \\ M &\quad s \quad c \\ &\quad \downarrow \\ F_{out} & \end{aligned}$$

$$\underline{E} \frac{\partial^2 u_d}{\partial x^2} + \rho \omega^2 u_d = 0 \quad (5)$$

in which  $\omega$  is the angular frequency,  $\rho$  is the density of the resilient layer,  $\underline{E} = E(1+j\eta)$  is the complex elastic modulus,  $\eta$  is the loss factor and  $u_d(x)$  is the amplitude of the harmonic one-direction displacement. The solution of equation (5) leads to following displacement, velocity  $v_d$  and pressure  $p_d$  distribution inside the resilient material:

$$p_d = Ae^{jk_d x} + Be^{-jk_d x} \quad (6)$$

$$v_d = j\omega u_d = -\frac{A}{Z_d} e^{jk_d x} + \frac{B}{Z_d} e^{-jk_d x} \quad (7)$$

where  $A$  and  $B$  are the amplitudes of the traveling waves in the negative and positive  $x$ -direction, respectively,  $k_d$  is the complex wave number of the longitudinal waves in the resilient material and  $Z_d$  is the complex impedance of the resilient material:

$$k_d = \frac{\omega}{\underline{c}_d} = \omega \sqrt{\frac{\rho}{E}} \approx \omega \sqrt{\frac{\rho}{E}} \left(1 - j\frac{\eta}{2}\right) \quad (8)$$

$$Z_d = \rho c_d = \sqrt{\rho E} \approx \sqrt{\rho E} \left(1 + j\frac{\eta}{2}\right) \quad (9)$$

The approximate expansions are valid for small loss factors ( $\eta \ll 1$ ).

Imposing the boundary conditions at the top of the resilient material ( $-\frac{F_m}{S} + p_d = j\omega M v_d$ ) and at the rigid bottom ( $v_d = 0$ ), the exact solution for the one-direction complex transmissibility  $\mathcal{T}_m$  becomes:

$$\mathcal{T}_m = \frac{1}{\frac{\omega M}{Z_d} \sin k_d L + \cos k_d L} \quad (10)$$

in which  $L$  is the thickness of the resilient component and  $M$  is the mass per unit area of the actual floating screed.

The above derivation deviates slightly from the original H-S-M model [9] where viscous damping was assumed. The result is however the same for small loss factors when the equivalent loss factor is determined from the viscosity  $\mu'$  as follows:  $\eta = \frac{\omega \mu'}{E}$ . Eq. (10) is then equivalent to the original H-S-M formula:

$$\mathcal{T}_m = \frac{1}{\cosh[(\alpha + j\beta) \cdot L] + \frac{j\omega M \cdot \sinh[(\alpha + j\beta) \cdot L]}{(\alpha + j\beta) \cdot (\frac{2\pi n}{\omega} - j\frac{E}{\rho})}} \quad (11)$$

with the damping parameter  $n = \frac{\eta}{2}$ , and the complex propagation function  $(\alpha + j\beta) = jk_d$ .

After a huge algebra, the square modulus of the force transmissibility  $|\mathcal{T}_m|^2$  can be derived from Eq. (11), and it is finally expressed as:

$$|\mathcal{T}_m|^2 = \frac{1 + 4n^2}{(1 + 4n^2) \cdot [\sinh^2(n\beta L) + \cos^2(\beta L)] + \frac{\omega}{\omega_0} \sqrt{\frac{M}{m}} \left(\frac{1}{1+n^2}\right) [n \sinh(2n\beta L) - (1 + 2n^2) \sin(2\beta L)] + \frac{\omega^2}{\omega_0^2} \frac{M}{m} \left(\frac{1}{1+n^2}\right) [\sinh^2(n\beta L) + \sin^2(\beta L)]} \quad (12)$$

where  $\omega_0 = \sqrt{\frac{E}{ML}}$  is the mass-spring-resonance frequency,  $m$  is the mass per unit area of the resilient layer (namely,  $m = \rho L$ ), and  $\beta L = \frac{\omega}{\omega_0} \sqrt{\frac{m}{M}}$ .

Eq. (12), being the analytical solution for  $|\mathcal{T}_m|$ , only depends on well-defined mechanical quantities, such as the mass per unit area of the actual floating screed  $M$ , the mass per unit area of the resilient layer  $m$ , the fundamental resonance frequency of the floating floor  $\omega_0$ , and the loss factor  $\eta$  of the resilient component. Relation (12) slightly differs from the original H-S-M equation [9].

In this way, once experimental values are accurately determined, it is possible to estimate the improvement of impact sound insulation of floating floors with an acoustically thick resilient layer, by applying  $\Delta L_m = 20 \log |1/\mathcal{T}_m|$ , as shown in Fig. 2.

The force transmissibility theory is a particular case of the H-S-M-model, in which the density and thickness of the resilient are small enough to disregard thickness-resonance wave effects. These effects involve an increase of the transmitted energy (therefore a decrease in the improvement of impact sound insulation), in correspondence with the resonance frequencies  $\omega_i$  of the standing waves in the resilient component of the system. The resonance frequencies are determined by:

$$\omega_i = \omega_0 i \pi \sqrt{\frac{M}{m}} \quad (\text{with } i = 1, 2, 3, \dots, n) \quad (13)$$

The corresponding values of  $\omega_i$  minimize the denominator of equation (12). Relation (13) is very useful, since it allows to immediately identify, as a function of the inertial and elastic properties of the materials, the frequency range in which thickness-resonance wave effects occur.

### 2.3. Consistency with existing empirical models

If the mass per unit area of the resilient component  $m$  is negligible with respect to the mass per unit area of the floating screed  $M$ , such as in ordinary floating floors (i.e.,  $m \ll M$ ), the resonance frequencies  $\omega_i$  of the standing waves, Eq. (13), occur at very high frequencies, beyond the frequency range of interest (>5 kHz). It follows that at the limit  $m \rightarrow 0$ , properly implying  $\rho L \rightarrow 0$ , and then  $(\alpha + j\beta)L \rightarrow 0$ , Eq. (11) is reduced to the ordinary transmissibility function for hysteretic damping, Eq. (4), as follows:

$$\lim_{m \rightarrow 0} |\mathcal{T}_m|^2 = \frac{1 + 4n^2}{4n^2 + \frac{(E - MLo^2)^2}{E^2}} = \frac{1 + 4n^2}{4n^2 + \left(1 - \left(\frac{\omega}{\omega_0}\right)^2\right)^2} = |\mathcal{T}|^2 \quad (14)$$

On the other hand, at the limit  $m \rightarrow M$ , the effects of thickness-resonant waves occur closely to the mass-spring resonance frequency of the floating floor, greatly reducing the efficiency of the system over the entire frequency range, as schematically shown in Fig. 3.

Moreover, if the dissipative term  $n$  is also neglected, i.e.,  $n \rightarrow 0$ ,  $\mathcal{T}_m$  from Eq. (14) can be simply rewritten as:

$$\lim_{m \rightarrow 0} \lim_{n \rightarrow 0} |\mathcal{T}_m|^2 = \frac{1}{\left(1 - \left(\frac{MLo^2}{E}\right)\right)^2} \quad (15)$$

Since  $\sqrt{E/ML} = \omega_0$ , Eq. (15) is reduced to the well-known Cremer-Vér formula in the usual form, as follows:

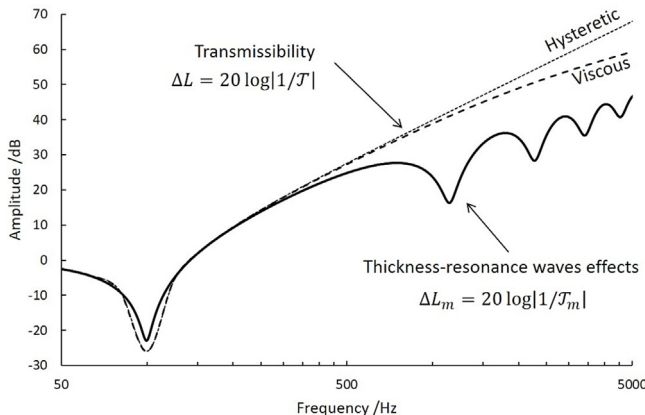


**Fig. 2.** Example of an estimation of the improvement of impact sound insulation by applying the ordinary transmissibility theory (thick dotted line, with viscous damping, Eq. (3); thin dotted line, with hysteretic damping, Eq. (4)), and by applying the revised H-S-M model (full line).

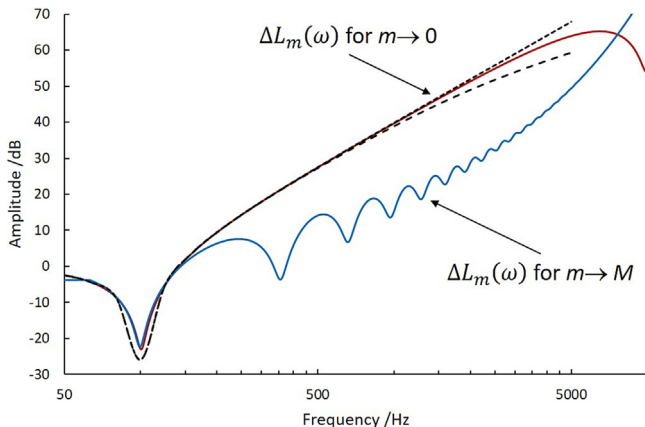


**Fig. 3.** Illustrative examples of  $\Delta L_m(\omega)$  calculated at the limit  $m \rightarrow 0$  (red curve), and at the limit  $m \rightarrow M$  (blue curve), compared with  $\Delta L(\omega)$  calculated from ordinary vibration transmissibility functions, Eq. (3) (thick dotted line), and Eq. (4), (thin dotted line). (For interpretation of the references to colour in this figure legend, the reader is referred to the web version of this article.)

$$\lim_{m \rightarrow 0} |\mathcal{T}_m|^2 = \lim_{n \rightarrow 0} |\mathcal{T}|^2 = \frac{1}{\left(1 - \left(\frac{\omega}{\omega_0}\right)^2\right)^2} \quad (16)$$

### 3. Experimental validation

#### 3.1. Experimental test procedure

To verify the effectiveness of the revised H-S-M model in predicting the effect of thickness-resonances on the acoustic performance of floating floors, six different types of resilient layers are investigated. Namely, three thick thermal layers, denoted as 'EPS', and three heavy resilient acoustic layers, denoted as 'EPDM'.

The EPS layers (samples 1, 2 and 3) consist of controlled expanded polystyrene granules mixed with cement, water and special additives. The EPDM layers (samples 4, 5 and 6) consist of rubber grains aggregate with natural polymer binders. The resilient layers are covered by a lightweight concrete finishing screed without any additional layer, except protective plastic foils. In Fig. 4 the configurations of the investigated floor systems, built with EPS thermal layers and EPDM resilient layers, are depicted.

The improvement of impact sound insulation  $\Delta L$  of samples 1, 2, 3 and 4 was measured in the frequency range of 50 Hz – 5 kHz according to the ISO Standard 10140 – series [12] in the acoustics laboratory of Buildwise. The floating floors were installed on a 140 mm concrete reference floor with a density of 2400 kg/m<sup>3</sup> and a surface area of 11.5 m<sup>2</sup>.  $\Delta L$  of samples 5 and 6 was measured in the acoustics standard laboratory of INRIM, in the frequency range of 100 Hz – 5 kHz, according to ISO Standard 140-6 (measurements performed before 2010) [21]. The floating floors were installed on a 140 mm concrete reference floor with a density of 2500 kg/m<sup>3</sup> and a surface area of 10 m<sup>2</sup>. Measurements were performed after 28 days of floating slab curing time. Since the standards ISO 140-6 and ISO 10140 series do not present substantial differences (for laboratory measurements of impact sound insulation), the results are considered compatible. In Fig. 5 the installation of the floating floors and the standard laboratories at Buildwise and at INRIM are shown.

#### 3.2. Material properties

The experimental values (with the related standard uncertainties) of the material properties of the floating floor systems are given in Table 1. The thickness of the EPS layers and the finishing screeds was measured at 5 randomly distributed locations. The density of the products was obtained by weighing 5 samples of different sizes. The measurements of the EPS density show a deviation of around 6% due to the inhomogeneity of the product. In Fig. 6 the evaluation of thickness and weight are depicted.

The apparent dynamic stiffness,  $s'_t$ , of the resilient materials was measured according to ISO 9052-1 [22] on 4 different samples for each type of resilient material. For the EPS samples, the measure-

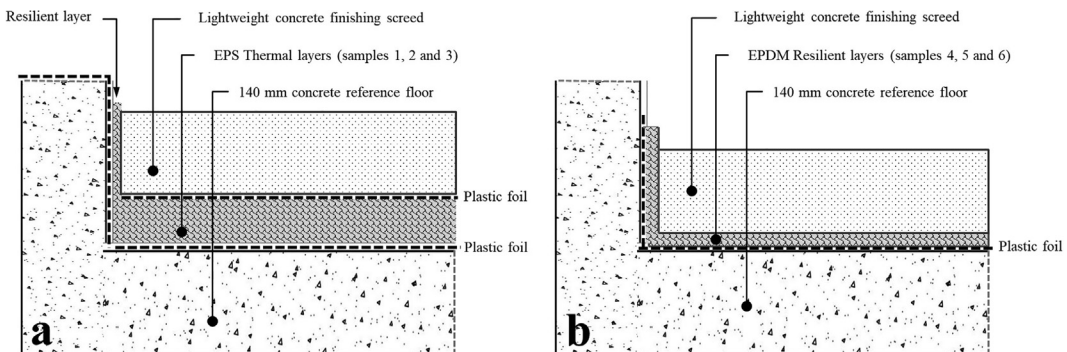


**Fig. 4.** The configuration of the floor systems investigated: a) floating floors with thermal EPS layers; b) floating floors with EPDM resilient layers.

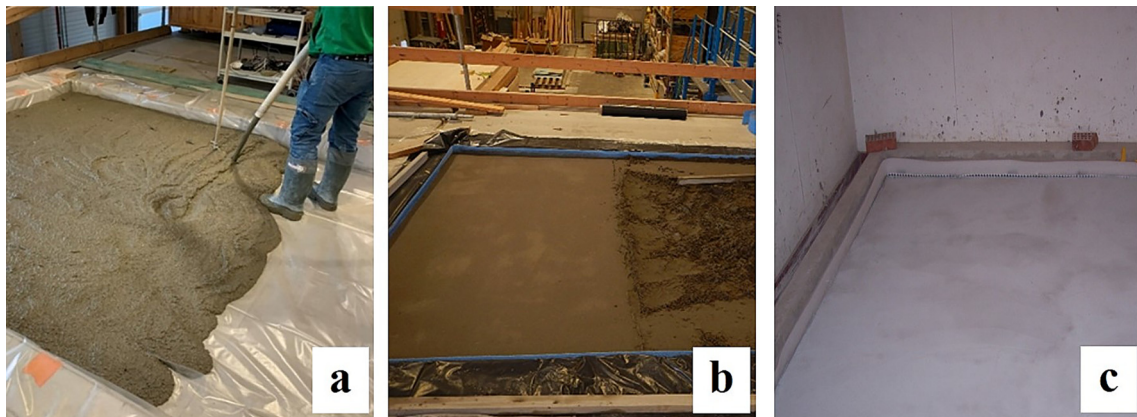


**Fig. 5.** a) Installation of the floating floor at Buildwise: application of the thermal layer composed of polystyrene foam granules (EPS), b) and the screed; c) lightweight finished screed applied on EPDM resilient layers at INRIM.

**Table 1**

Material properties: experimental values and standard uncertainties.

	Thermal/resilient layer				Finishing screed	
	$\rho / \text{kg} \cdot \text{m}^{-3}$	$L / \text{mm}$	$\eta / -$	$s'_t / \text{MN} \cdot \text{m}^{-3}$	$\rho / \text{kg} \cdot \text{m}^{-3}$	$L / \text{mm}$
1	EPS 330–50 mm	$327 \pm 19$	$48 \pm 2$	$0.16 \pm 0.03$	$150 \pm 16$	$1930 \pm 140$
2	EPS 330–100 mm	$327 \pm 19$	$93 \pm 3$	$0.22 \pm 0.03$	$195 \pm 10$	$1930 \pm 140$
3	EPS 180–100 mm	$180 \pm 9$	$100 \pm 6$	$0.20 \pm 0.03$	$197 \pm 4$	$1930 \pm 96$
4	EPDM rubber 6 mm	$950 \pm 48$	$6 \pm 0.4$	$0.50 \pm 0.07$	$57 \pm 11$	$1800 \pm 90$
5	EPDM (rubber grains)	$550 \pm 23$	$15 \pm 2$	$0.20 \pm 0.02$	$32 \pm 6$	$1660 \pm 160$
6	EPDM (rubber shavings)	$400 \pm 18$	$20 \pm 3$	$0.22 \pm 0.02$	$27 \pm 5$	$1750 \pm 170$

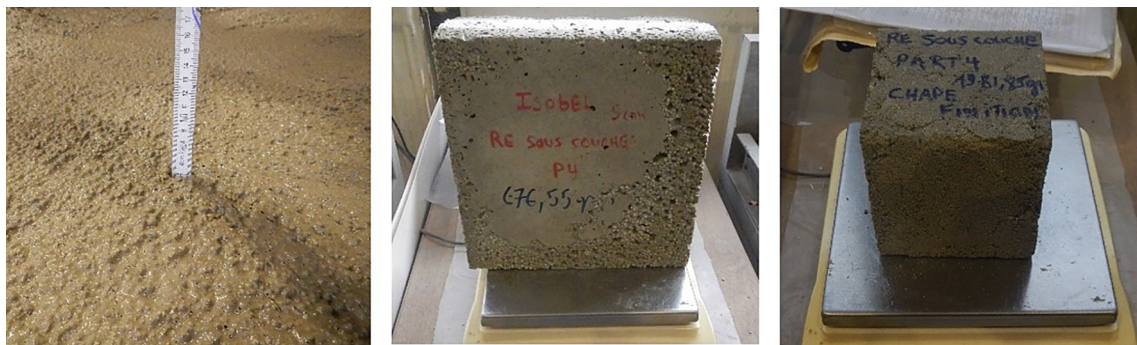


**Fig. 6.** Illustration of thickness and density measurements.

ments were carried out after a loading period of 28 days in order to be consistent with the  $\Delta L$  measurements carried out after a screed drying period of 28 days. For the EPDM samples, the measurements were carried out after 3 days: the long-term dynamic stiffness values were extrapolated at 30 days, by applying the creep-based calculation model, as described in [23]. The loss factor  $\eta$  of the resilient components was determined from the width of the experimental resonance peak  $\omega_r$  by applying the half-power bandwidth method,  $\eta = \Delta\omega/\omega_r$ . For the EPS samples, the measurements show a deviation of 2 to 11% on the dynamic stiffness and a deviation of 12 to 21% on the loss factor. For the EPDM samples, the deviation is up to 20% for the dynamic stiffness and 9 to 14 % for the loss factor. In Fig. 7 the test-rigs of dynamic stiffness measurements are shown.

For simple elastic layers, the dynamic stiffness depends on the Young's modulus and its thickness ( $s = E/L$ ). Contrary to what is predicted by theory, EPS sample 2 with thickness 100 mm has a higher dynamic stiffness than sample 1 with thickness 50 mm,

meaning that the Young's modulus is not a constant material property. This is due to the inhomogeneity of the mix and the greater compaction of the product for larger thicknesses.

### 3.3. Application of revised H-S-M model and comparison with experimental data

The H-S-M model is applied to estimate the improvement of impact sound insulation of the floating floors described in the previous section. As a first step, from the experimental data collected in Table 1, it is possible to calculate the fundamental mass-spring-resonance frequency  $f_0 = \frac{1}{2\pi} \sqrt{\frac{s'}{M}}$  the thickness-resonance frequencies of standing waves  $f_i = f_0 i \pi \sqrt{\frac{M}{m}}$  in the resilient component, as indicated in Table 2. Here, M is the mass per unit area of the actual floating screed and m is the mass per unit area of the thermal and resilient layers. For the floating floors investigated, the standing

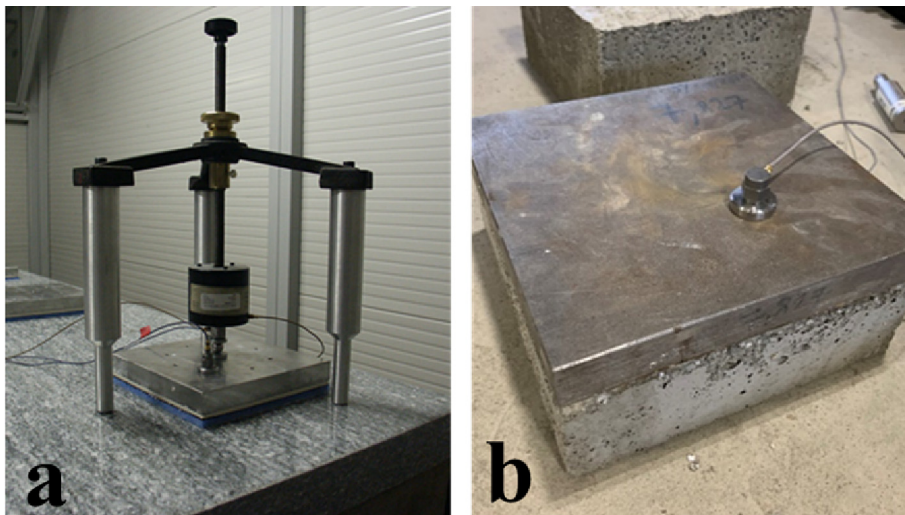


**Fig. 7.** Illustration of the apparent dynamic stiffness and loss factor measurements test-rigs: a) the experimental set-up developed at INRIM; b) the experimental set-up used at Buildwise.

**Table 2**

Calculated resonance frequencies in Hz of the floating floors and the estimated standard uncertainties.

		$f_0$	$f_1$	$f_2$	$f_3$	$f_4$	$f_5$
1	EPS 330–50 mm	<b>202 ± 31</b>	1545 ± 261	3091 ± 523	4637 ± 784	> 5000	–
2	EPS 330–100 mm	<b>230 ± 34</b>	1266 ± 205	2532 ± 410	3798 ± 616	> 5000	–
3	EPS 180–100 mm	<b>207 ± 33</b>	1654 ± 279	3308 ± 557	4962 ± 836	> 5000	–
4	EPDM rubber 6 mm	<b>124 ± 18</b>	1581 ± 250	3162 ± 500	4743 ± 750	> 5000	–
5	EPDM (rubber grains)	<b>566 ± 58</b>	984 ± 98	1969 ± 197	2954 ± 296	3938 ± 395	> 5000
6	EPDM (rubber shavings)	<b>555 ± 57</b>	918 ± 92	1837 ± 184	2755 ± 277	3674 ± 369	> 5000

waves occur within the frequency range of interest for impact sound (<5000 Hz).

The measured impact sound insulation improvements  $\Delta L$ , in one-third octave bands, are compared with predictions on the basis of the revised H-S-M model in Fig. 8 for the configurations with thick EPS thermal layers. Reference predictions with the

transmissibility model for acoustically thin layers according to Eq. (4) are also shown. In the graphs the maximum admissible range, the absolute minima and absolute maxima among all values (at a confidence level of 95 %) calculated according to Appendix A, are also indicated for the H-S-M predictions. For the measurements, the expanded uncertainty for a confidence level of 95 %

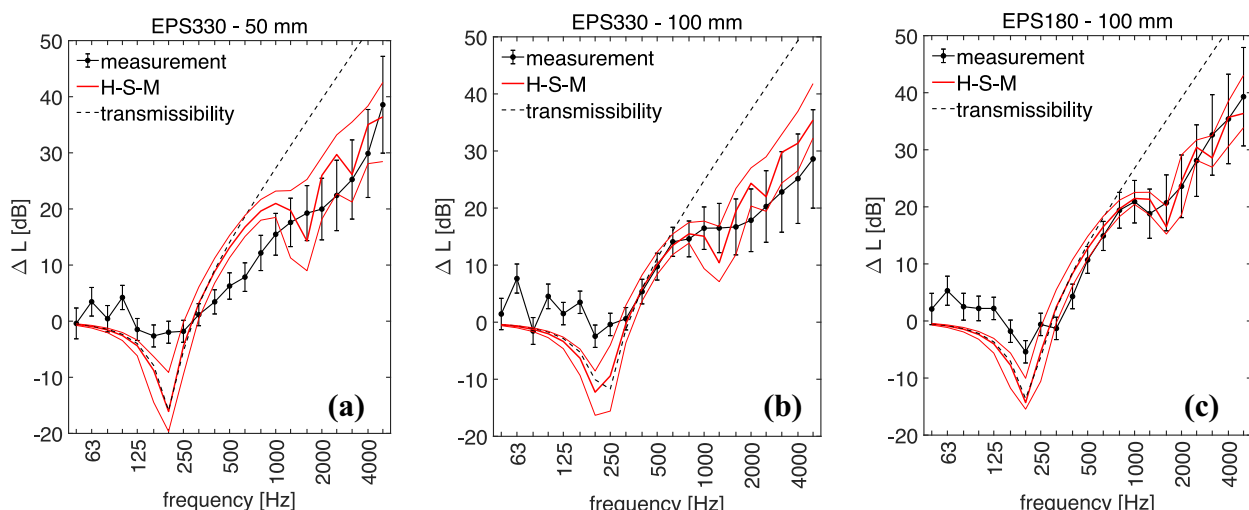


**Fig. 8.** Measured  $\Delta L$  (bullets points), the estimated  $\Delta L$  according to the transmissibility model of Eq. (4) (dotted line) and the estimated  $\Delta L$  according to the revised H-S-M model (red thick line) with the admissible range (red thin lines), for floating floors with a thick thermal resilient layer (a) type 1, (b) type 2, and (c) type 3. (For interpretation of the references to colour in this figure legend, the reader is referred to the web version of this article.)

( $k = 2$ , two-sided) is shown using the standard uncertainties at reproducibility conditions for the reduction in impact sound pressure level of ISO 12999-1 [24].

The thickness-wave effects reduce the impact noise insulation of the floating floor in the medium and high frequencies by as much as 20 dB below what would be expected from the transmissibility model. The H-S-M model predicts the frequency position of the resonances (mass-spring resonance and thickness-wave resonances) relatively well, but the estimated average data show more pronounced resonance dips compared to the measured data. Furthermore, the slope of the 50 mm EPS curve above the mass-spring resonance frequency, as shown in Fig. 8a, is not well predicted, particularly in the mid frequency range. Discrepancies could possibly be related to different dissipative properties of the actual floating screeds, slightly affecting the amplitude of the input force. In the proposed model, the input force is supposed to be completely transmitted to the resilient material below, by considering the motion of the floating screed as totally free. In the laboratory experiments, the constrained conditions (discussed in Section 4.1) limiting the free lateral expansions of the resilient layer [25], the frictional effects (here not taken into account) due to the lateral couplings [26], and the base floor mobility (discussed in Section 4.2 and in Appendix B), affect the mechanical response of the system, and thus the related sound radiation. Moreover, it is possible that the H-S-M model does not adequately handle the effect of the two distinct types of damping: the hysteretic damping which acts more on the resonance peaks and the viscous damping which acts more on the slope.

In Fig. 9, results for the configurations with heavy EPDM resilient layers are shown. The H-S-M model predicts the resonance frequencies positions quite well, although both the mass-spring-resonance frequency and the first thickness resonance frequency are underestimated for floating floor type 4 (Fig. 9a). Discrepancies between predictions and experimental results can be attributed to constrained conditions, to dissipative effects within the actual floating screeds, to the base floor mobility, and to hysteretic and viscous damping behavior, as previously discussed.

In any case, it should be noted that the estimation of the reduction of impact sound insulation, obtained on the basis of a purely mechanical model, can be considered effectively satisfactory, for both thick and heavy layers investigated in this work. More specifically, the H-S-M model is particularly useful for comparing, at the

building physics design level, several combinations of involved materials, in order to achieve the more effective acoustic and thermal comfort, on the basis of suitable mechanical properties.

#### 4. Numerical validation with the transfer matrix method

##### 4.1. Influence of the constrained conditions in the lateral direction

The original H-S-M model was intended for isolation mounts for which the diameter is small compared to the wavelength. The one-dimensional derivation is not exact due to the presence of lateral waves. To validate the analytical H-S-M model when applied to infinite layers, results are compared with a detailed calculation by means of the transfer matrix method (TMM) [27]. For the TMM calculations, the MATLAB® application WinLayers [28] was used. In this application, the improvement in impact sound insulation  $\Delta L$  is calculated from the resulting sound pressure levels beneath the point-excited floors with and without floating screed.

The wave velocity  $c_d$  of the longitudinal waves in the resilient layer will be affected by the constrained conditions in the lateral direction of the resilient layer. In the infinite layer, the longitudinal waves will travel with the P-wave velocity:

$$c_d = \sqrt{\frac{E}{\rho} \frac{(1+\nu)}{(1-\nu)(1-2\nu)}} \quad (17)$$

with  $\nu$  the Poisson ratio of the resilient material. The influence of the infinite layer can thus be accounted for by using the constrained Young's modulus  $E_c = E \frac{(1+\nu)}{(1-\nu)(1-2\nu)}$  in the H-S-M model.

Fig. 10a compares the H-S-M model results for the floor system with resilient layer type 1 with the TMM reference solution for different values of the Poisson ratio. The constrained Young's modulus  $E_c$ , used as input in the H-S-M model, was kept constant ( $E_c = s'_L L = 7.2 \text{ MPa}$ ), while varying the Young's modulus  $E$  which is used as input in the TMM together with the corresponding Poisson ratio. The H-S-M model assumption of one-dimensional longitudinal wave propagation in the thermal layer is not valid in the entire frequency range of interest. The presence of shear waves leads to an anti-resonance peak, visible in the TMM results, at approximately 910 Hz for  $\nu = 0.20$ . The peak shifts to lower frequencies when the Poisson ratio increases. The effect is more important for the thicker resilient layer type 2 (Fig. 10b). For high

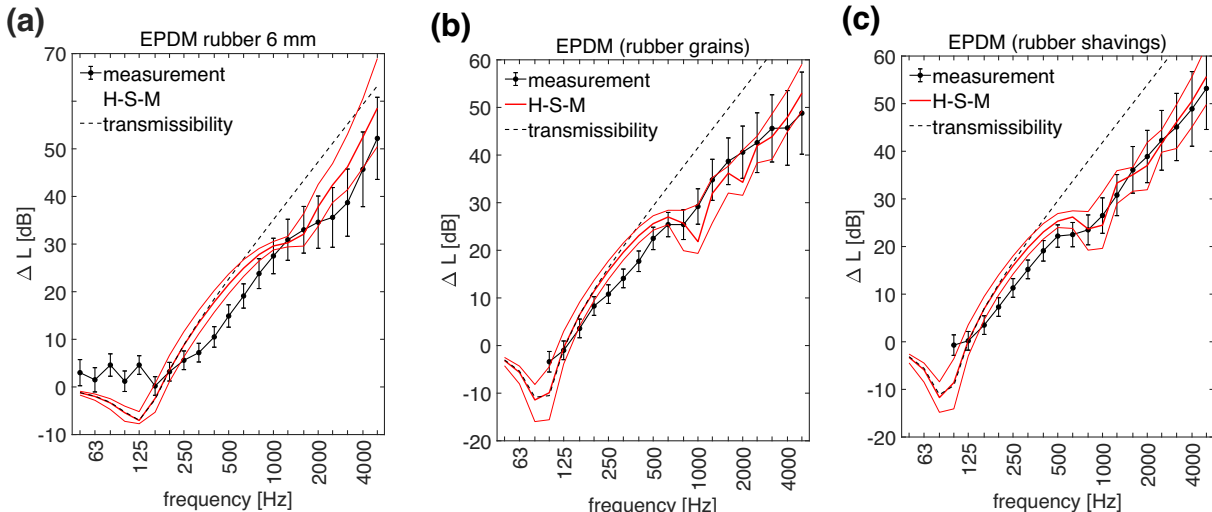


**Fig. 9.** Measured  $\Delta L$  (bullets points), the estimated  $\Delta L$  according to the transmissibility model of Eq. (4) (dotted line) and the estimated  $\Delta L$  according to the revised H-S-M model (red thick line) with the admissible range (red thin lines), for floating floors with a thin, heavy elastic interlayer (a) type 4, (b) type 5 and (c) type 6. (For interpretation of the references to colour in this figure legend, the reader is referred to the web version of this article.)

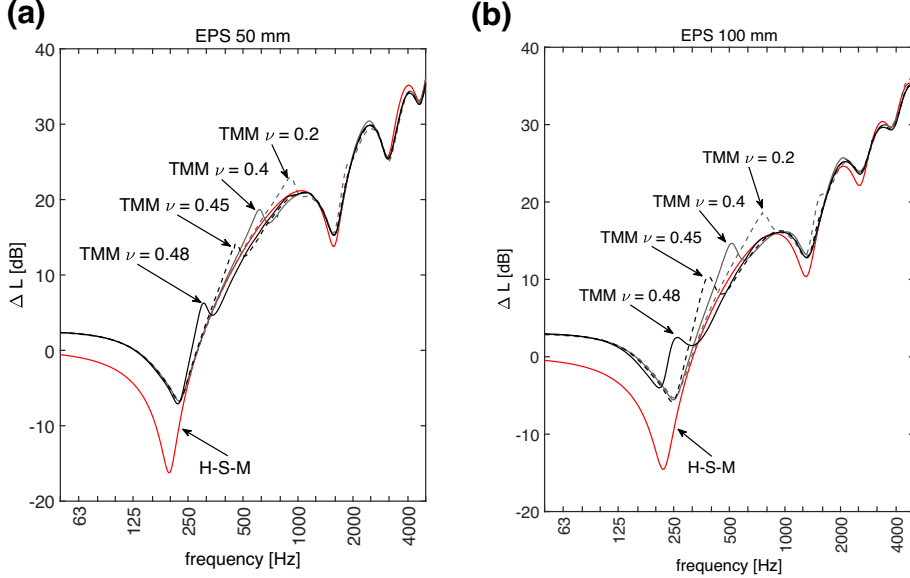


**Fig. 10.** Comparison between the H-S-M model and TMM results for the floor systems with a thick thermal resilient layer (a) type 1 and (b) type 2.

Poisson ratios and thick resilient layers, this anti-resonance effect can interfere with the mass-spring resonance dip of the system. Nevertheless, the agreement between the analytical H-S-M model and the TMM is very good above the mass-spring resonance frequency of the system. Below and around the mass-spring resonance frequency of the system, the force transmissibility model underestimates the improvement in impact sound insulation because the influence of the base floor mobility is not accounted for.

#### 4.2. Influence of base floor mobility

The constitutive models assume a rigid base floor and calculate the improvement in impact sound insulation  $\Delta L$  from the force transmissibility ratio  $\mathcal{T}$ . This approach neglects the mobility of the base floor. While the mobility can be disregarded at high frequencies, it has a significant effect below and around the mass-spring resonance frequency of the floating floor systems.

The base floor mobility influences the improvement of impact sound insulation in two ways. Below the resonance frequency, the floor system behaves as a single floor system and its impact sound insulation is largely determined by the mass per unit area of the floor system. The additional mass of the floating floor system will lead to an improvement in the impact sound insulation below the resonance frequency. This phenomenon is not accounted for in the force transmissibility models. Secondly, the mass per unit area of the base floor  $M_2$  will shift the resonance frequency of the system to higher frequencies, according to the formula for the resonance frequency of a mass-spring-mass system:

$$\omega_0 = \sqrt{s\left(\frac{1}{M_1} + \frac{1}{M_2}\right)} = \sqrt{s\left(\frac{M_1 + M_2}{M_1 M_2}\right)} \quad (18)$$

in which  $M_1 = M$  is the mass of the floating screed.

The H-S-M model can be adapted to incorporate the mobility of the base floor (Appendix B). By including the base floor mobility,

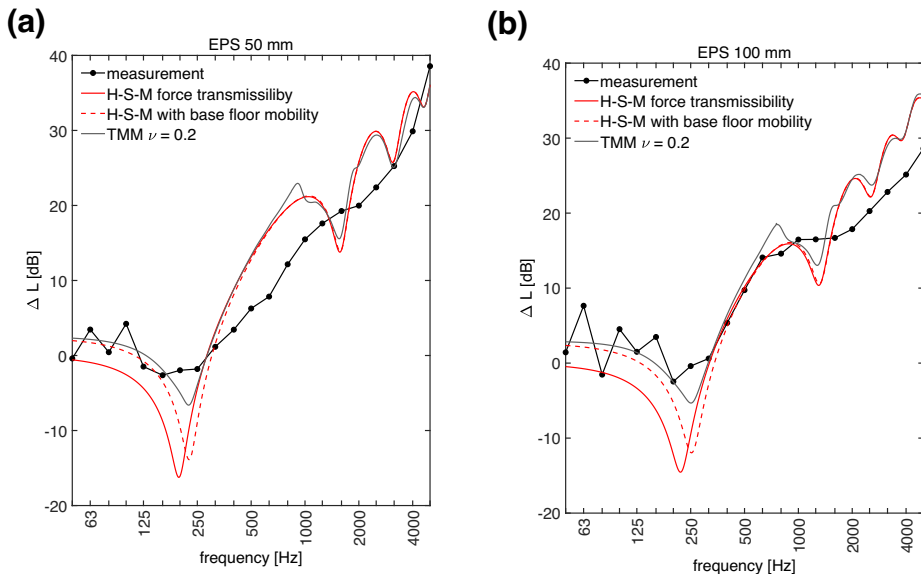


**Fig. 11.** Influence of base floor mobility in the H-S-M model for the floor systems with a thick thermal resilient layer (a) type 1 and (b) type 2.

the H-S-M model agrees better with the reference TMM solution and the measurement results at low frequencies (Fig. 11). The additional mass of the floating floor ( $M_1 + m$ ) leads to an improvement in impact sound insulation of  $20 \lg \frac{M_2+M_1+m}{M_2} = 2.4 \text{dB}$  when  $f \ll f_0$ . The shift in the resonance frequency (from 200 Hz to 230 Hz for 50 mm EPS and from 220 Hz to 255 Hz for 100 mm EPS) is also well predicted by the adapted model. However, the analytical model still underestimates the improvement in impact sound insulation around the mass-spring resonance dip. The constraint of the resilient layer in the lateral direction will increase the damping at the resonance frequency [26], which is not taken into account in the analytical model.

## 5. Conclusions

The mechanical model of Harrison-Sykes-Martin, revised and corrected, is applied to estimate the acoustical performance of floating floors in dwellings, built with thick or heavy elastic layers, used for thermal and acoustic insulation. The presented model provides a more detailed estimation of the acoustical performance of floating floors, with respect to existing analytical models, since the effect of thickness wave resonances on  $\Delta L$  is incorporated.

In order to be validated, the theoretical model is compared with measurement results obtained in two standard laboratories for three EPS thermal layers and three rubber-based acoustic layers. The input data for the model are derived from experimental measurements of apparent dynamic stiffness, loss factor, and surface mass of the resilient/thermal layer and surface mass of the floating screed. The simulations and experiments generally show a good compatibility: the model is able to identify the thickness-wave resonances fairly well, although the effect of damping is not well handled. The model accuracy is affected by the proper determination of the material parameters. Particular care should be taken when determining the dynamic stiffness according to ISO 9052-1. The boundary conditions in the small-scale measurement set-up do not correspond to the actual constrained boundary conditions in situ and may have a strong influence for certain types of resilient or thermal layers. Furthermore, the elastic material parameters can vary strongly with time and frequency (e.g. polyurethane). Frequency dependent material properties cannot be incorporated directly in the analytical H-S-M model.

A numerical validation with the transfer matrix method allows a deeper understanding of the physical phenomena involved. The H-S-M model assumption of one-dimensional longitudinal wave propagation in the thermal layer is not valid in the entire frequency range of interest. Furthermore, the TMM results agree better with measurements below and around the mass-spring resonance frequency compared with the force transmissibility models. The difference is caused by the influence of the base floor on  $\Delta L$  at low frequencies. The H-S-M prediction can be improved below the resonance frequency of the mass-spring system by accounting for the mobility of the base floor.

Nevertheless, the proposed analytical model allows, at the building physics design level, to identify suitable and optimized solutions for acoustical and thermal insulation, by opportunely combining the properties of involved materials. Moreover, it can be applied to identify in advance the acoustical performance of different typologies of resilient materials, in comparative survey tests and in quality product management.

## Data availability

Data will be made available on request.

## Declaration of Competing Interest

The authors declare that they have no known competing financial interests or personal relationships that could have appeared to influence the work reported in this paper.

## Appendix A. Model sensitivity and uncertainty budget

To evaluate the impact of the single input parameters on the model, i.e. the model sensitivity and the expanded uncertainty associated with the improvement of impact sound insulation  $U(\Delta L_m(\omega))$  as function of frequency, the general rule of GUM [29] uncertainty propagation is applied. By considering all input variables as independent (by excluding the floating floor resonance frequency  $\omega_0$ , depending on the comprehensive elastic modulus  $E$  of the resilient component), the model sensitivity assessment and the expanded uncertainty is based on the following relation:

$$U(\Delta L_m(\omega)) = k \cdot \sqrt{\sum_{i=1}^N \left( \frac{\partial \Delta L_m(\omega)}{\partial x_i} \right)^2 u^2(x_i)} \quad (\text{A.1})$$

in which  $k$  is the coverage factor (namely,  $k = 2$  provides an interval having a confidence level of approximately 95%),  $\partial \Delta L_m(\omega) / \partial x_i$  is the sensitivity coefficient,  $\Delta L_m(\omega)$  is the relation  $20 \log |1/\mathcal{T}_m|$ , where  $|\mathcal{T}_m|$  is given in Eq. (12),  $x_i$  is the  $i^{\text{th}}$  independent variable of Eq. (12), and  $u^2(x_i)$  is the standard uncertainty, associated with the independent variable  $x_i$ . It should be noted that  $\Delta L_m(\omega)$  is a function of frequency  $\omega = 2\pi f$ , in the range between 50 Hz and 5000 Hz.

The independent variables in Eq. (12) are the dissipative coefficient  $n = \eta_c/2$ , the mass per unit area of the resilient component  $m$ , and the mass per unit area of the floating screed  $M$ . In order to take into account also the variability of the floating floor resonance frequency  $\omega_0$ , relation (A.1) is independently calculated for  $\omega_0 + 2\sigma_{\omega_0}$  (namely,  $\Delta L_{m,1}(\omega)$ ), and for  $\omega_0 - 2\sigma_{\omega_0}$  (namely,  $\Delta L_{m,2}(\omega)$ ), where  $\sigma_{\omega_0}$  is the experimental standard deviation, obtained by the repeatability and reproducibility of the measured elastic properties (in terms of dynamic stiffness  $s$ ) of the resilient component. Finally, to calculate the maximum admissible range, the absolute minima and absolute maxima among all values (at a confidence level of 95 %) are pointed out:

$$\Delta L_{m,\min}(\omega) = \min [\Delta L_{m,1}(\omega) - U_1(\Delta L_{m,1}(\omega)), \Delta L_{m,2}(\omega) - U_2(\Delta L_{m,2}(\omega))] \quad (\text{A.2})$$

$$\Delta L_{m,\max}(\omega) = \max [\Delta L_{m,1}(\omega) + U_1(\Delta L_{m,1}(\omega)), \Delta L_{m,2}(\omega) + U_2(\Delta L_{m,2}(\omega))] \quad (\text{A.3})$$

Relations (A.2) and (A.3) provide the overall expected upper and lower limit of the model at a confidence level of 95 %, as a function of material properties and related experimental uncertainties.

## Appendix B. Including the effect of base floor mobility

### B.1 Constitutive model for acoustically thin resilient layer (hysteretic damping)

The effect of the base floor mobility can be incorporated in the classic constitutive model by looking at the velocity of the base floor instead of the force (Fig. B.1). The ratio of the velocities of the base floor in the cases without and with floating floor can be calculated using the mobility approach [1]:

$$\frac{v_2}{v_{2,0}} = \frac{Z_d F_{in}}{Z_1 Z_2 + Z_d(Z_1 + Z_2)} \cdot \frac{Z_2}{F_{in}} = \frac{Z_d}{Z_1 + Z_d(1 + \frac{Z_1}{Z_2})} \quad (\text{B.1})$$

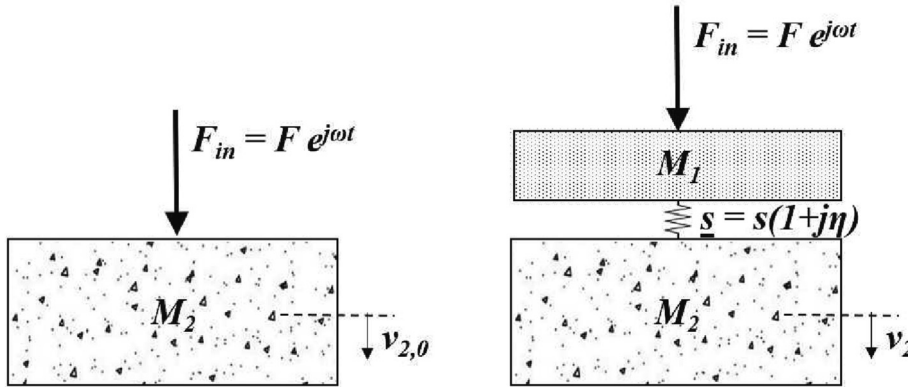


**Fig. B1.** Model for calculating the improvement of impact sound insulation by a single resilient floating floor (floating screed with mass per unit area  $M_1$ , resilient layer with dynamic stiffness  $s$  and total loss factor  $\eta$ ) incorporating the effect of the mobility of the base floor (mass per unit area  $M_2$ ).

where  $Z_1$ ,  $Z_2$  and  $Z_d$  are the impedance of the floating screed, the base floor and the resilient layer, respectively. Modelling the floating screed and base floor as a mass with impedance  $Z = j\omega M$  and using the impedance of the resilient layer with complex dynamic stiffness  $Z_d = -\frac{js}{\omega}$ , the velocity ratio equals:

$$\frac{v_2}{v_{2,0}} = \frac{-\frac{js}{\omega}}{j\omega M_1 - \frac{js}{\omega} \left( \frac{M_1+M_2}{M_2} \right)} \quad (\text{B.2})$$

By assuming that the radiated power from the base floor is proportional to the velocity squared, it follows

$$\Delta L_v = 20 \log \left| \frac{v_{2,0}}{v_2} \right| = 20 \log \sqrt{\frac{\eta^2 \left( \frac{M_1+M_2}{M_2} \right)^2 + \left( \frac{M_1+M_2}{M_2} - \frac{\omega^2}{\omega_0^2} \right)^2}{1 + \eta^2}} \quad (\text{B.3})$$

with  $\omega_0 = \sqrt{\frac{s}{M_1}}$ . When  $M_2 \gg M_1$ , this relation simplifies to Eq. (4).

## B.2 Harrison-Sykes-Martin model (hysteretic damping)

The H-S-M model of section 2.2 can be adapted to incorporate the mobility of the base floor by solving the differential equation (5) with the appropriate boundary condition. The masses at the boundaries (bottom,  $x = 0$ , and top,  $x = L$ ) impose the following boundary conditions:

$$-p_d(0) = j\omega M_2 v_d(0) \quad (\text{B.4})$$

$$-\frac{F_{in}}{S} + p_d(L) = j\omega M_1 v_d(L) \quad (\text{B.5})$$

The unknown amplitudes  $A$  and  $B$  in Eqs. (6)-(7) can be determined from these two boundary conditions. The condition at  $x = L$  gives:

$$B = \frac{j\omega M_2 - Z_d}{j\omega M_2 + Z_d} A \quad (\text{B.6})$$

In the original H-S-M model, the rigid boundary condition leads to a perfect reflection ( $|B| = |A|$ ). After a considerable amount of algebra, the first boundary condition results in the following relation for the ratio of the base floor velocities with and without floating floor:

$$\frac{v_2}{v_{2,0}} = \frac{1}{\frac{-\omega M_1}{Z_d} \sin k_d l + \frac{M_1+M_2}{M_2} \cos k_d l + \frac{Z_d}{\omega M_2} \sin k_d l} \quad (\text{B.7})$$

The improvement in impact sound insulation can again be calculated from  $\Delta L_{m,v} = 20 \log \left| \frac{v_{2,0}}{v_2} \right|$ .

## References

- [1] Cremer L. Theorie des Klopfshalles bei Decken mit Schwimmenden Estrich. *Acust* 1952;2:167–8.
- [2] Vér I. Impact noise isolation of composite floors. *J Acoust Soc Am* 1971;50 (4A):1043–50.
- [3] ISO 12354-2:2017. Building acoustics – Estimation of acoustic performance of buildings from the performance of elements – Part 2: Impact sound insulation between rooms.
- [4] Den Hartog J P. Mechanical vibrations. 1934, 1<sup>st</sup> ed., McGraw-Hill Book Company, Inc. e New York.
- [5] Schiavi A. Improvement of impact sound insulation: a constitutive model for floating floors. *Appl Acoust* 2018;129:64–71.
- [6] Henderickx F, Mertens C. Rigidité dynamique et transmission acoustique des bruits de choc. *CSTC revue* 1988;4:50–61.
- [7] Crispin C, Wuyts D, Dijckmans A. Thickness-resonance waves in underlays of floating screed. *INTER-NOISE and NOISE-CON Congress and Conference Proceedings*, Washington, D.C., 2021.
- [8] Harrison M, Sykes AO, Martin M. Wave effects in isolation mounts. *J Acoust Soc Am* 1952;24:62–71.
- [9] Harrison M, Sykes AO, Martin M. Wave effects in isolation mounts. revised ed. Washington, DC: The David W. Taylor Model Basin; 1964.
- [10] Snowdon JC. Vibration and shock in damped mechanical systems. John Wiley & Sons Inc; 1968.
- [11] Du Y, Burdisso R, Nikolaidis E, Tiwari D. Effects of isolators internal resonances on force transmissibility and radiated noise. *J Sound Vib* 2003;268(4):751–78.
- [12] ISO 10140 – (all parts): 2021. Acoustics – Laboratory measurement of sound insulation of building elements.
- [13] Gerretsen E. Calculation of airborne and impact sound insulation between dwellings. *Appl Acoust* 1986;19(4):245–64.
- [14] Vigran T. Building acoustics. Oxon: Taylor & Francis; 2008.
- [15] Arenas JP, Castaño JL, Troncoso L, Auad ML. Thermoplastic polyurethane/laponite nanocomposite for reducing impact sound in a floating floor. *Appl Acoust* 2019;155:401–6.
- [16] Hongisto V, Virjonen P, Maula H, Saarinen P, Radun J. Impact sound insulation of floating floors: A psychoacoustic experiment linking standard objective rating and subjective perception. *Build Environ* 2020;184:107225.
- [17] Wang J, Du B. Experiment on the optimization of sound insulation performance of residential floor structure. *Appl Acoust* 2021;174:107734.
- [18] Jabłoński M, Bednarska D, Grymin W, Schiavi A, Konioczyk M. Prediction for the acoustic performance of a floating floor: Novel probabilistic approach considering materials Gaussian uncertainties. *Appl Acoust* 2021;182:108252.
- [19] Arenas JP, Sepulveda LF. Impact sound insulation of a lightweight laminate floor resting on a thin underlayment material above a concrete slab. *J Build Eng* 2022;45:103537.
- [20] Gibson B, Nguyen T, Sinaie S, Heath D, Ngo T. The low frequency structure-borne sound problem in multi-storey timber buildings and potential of acoustic metamaterials: a review. *Build Environ* 2022;109531.
- [21] ISO 140-6:1998. Acoustics – Measurement of sound insulation in buildings and of building elements – Part 6: Laboratory measurements of impact sound insulation of floors (Withdrawn).
- [22] ISO 9052-1:1989. Acoustics – Determination of dynamic stiffness – Part 1: Materials used under floating floors in dwellings.
- [23] Schiavi A, Belli AP, Corallo M, Russo F. Acoustical performance characterization of resilient materials used under floating floors in dwellings. *Acta Acust united Ac* 2007;93(3):477–85.
- [24] ISO 12999-1:2020. Acoustics - Determination and application of measurement uncertainties in building acoustics - Part 1: Sound insulation.
- [25] Meyer Z, Olszewska M. Methods development for the constrained elastic modulus investigation of organic material in natural soil conditions. *Materials* 2021;14(22):6842.

- [26] Marino L, Cicirello A, Hills DA. Displacement transmissibility of a Coulomb friction oscillator subject to joined base-wall motion. *Nonlinear Dyn* 2019;98(4):2595–612.
- [27] Allard J, Atalla N. Propagation of sound in porous media. modelling sound absorbing materials. 2nd ed. Chichester: John Wiley & Sons Ltd; 2009.
- [28] Gebelein N. Structure-borne sound sensitivity of building structures. Assessment of the acoustic performances of multi-layered structures by simulation and measurement techniques. Leuven: Katholieke Universiteit Leuven; 2008. PhD thesis.
- [29] JCGM 100. Evaluation of measurement data – guide to the expression of uncertainty in measurement. France: Joint Committee for Guides in Metrology, Sèvres (GUM); 2008.